Kuwait J.Sci., Vol.49, No.(1),January.2022,pp(1-14)

Linear and nonlinear low-frequency collisional quantum Buneman Instability in electron-positron-ion Plasmas

M. Nasir Khattak[1,] *, U. Zakir[2], M. Yaqoob Khan[3], Niaz. Wali[4] & Tariq. Jan [5]

[1]*Dept. of Physics, Khushal Khan Khattak University Karak, 27300, Khyber Pakhtunkhwa, Pakistan.*
[2]*Dept. of Physics, University of Malakand Dir (L), Khyber Pakhtunkhwa, 18800 Pakistan.*
[3]*Dept. of Physics, Kohat University of Science & Technology Kohat, 46000, Khyber Pakhtunkhwa Pakistan.*
[4]*Institute for Fusion Theory and Simulation, Department of Physics, Zhejiang University, Hangzhou, 310027, China.*
[5]*ORIC Dept., Kohat University of Science & Technology Kohat, 46000, Khyber Pakhtunkhwa Pakistan*

[*]*Corresponding author: mnnasirphysics@gmail.com*

Abstract

The linear and nonlinear low-frequency collisional quantum Buneman instability in electron-positron-ion plasmas have been studied. Buneman instability in low frequency three species quantum plasma has been investigated using the approach of the quantum hydrodynamic model. The one-dimensional low-frequency collisional model is revisited by introducing the Bohm potential term in the momentum equation along with the role of the positron. Low-frequency Buneman instability which arises by one stream of particles drifting over another is investigated in the presence of the positron. Different plasma configurations based on the relative velocities of streaming particles are analyzed and it is observed that positron content enhances the instability in classical limits. Further, we found that in pure quantum limits the instability growth rate is decreased by increasing the positron concentration. The present work is very useful for the nonlinear problems in Quantum Coulomb systems.

Keywords: Growth rate; Bohm potential; Buneman instability; quantum plasma; two stream Instability:

1. Introduction

The relative motion of plasma particles e.g., ions and electrons are considered as a main source of streaming in plasma. Buneman instability in classical plasmas is the fundamental process of instability. Buneman instability which is also called Farley Buneman instability was first studied theoretically in the late Fifties by Buneman and Farley (Buneman, 1959; Buneman, 1958; Inhester *et al*., 1981; Niknam *et al.,* 2011). This instability arises when it is a significant drift

difference between ions and electrons. This comparative drift velocity difference is somewhat greater than the electron thermal velocity i.e. $V_t = \frac{qKB\,Te}{me}$, here $V_t$is the thermal velocity of electrons, K_B is Boltzmann constant, and I am the electron mass (Niknam *et al*., 2011; Haas & Bret, 2012). Streaming develops because of the relative motion of electrons and ions (Shokri & Niknam, 2005). The contribution of the stationary ions in two-stream instability leads to Buneman instability when the current stream crosses the magnetized plasmas. Ions are supposed to behave stationery and electrons are assumed to flow with larger velocity across the ion fluid. In this case, weakly ion-acoustic instability occurs as the electron thermal velocity turns out to be more than the relative streaming velocity between ions and electrons. However, when the drift velocity of ions and electrons is larger than the thermal velocity of the electrons, in such situations the electron-ion deeply growing two-stream instability turns into Buneman instability (Jun & Bin, 2012). Buneman instability has been the focus of various studies in recent years (Madsen *et al*., 2012; Haas *et al*., 2012; Bandara & Khachan, 2015; Pandey *et al*., 2014; Hong *et al.,* 2015), due to its important role in the solar chromosphere (Madsen *et al*., 2014), earth ionosphere (Dolgov *et al*., 2014), in Lorentz dusty plasma (Ki & Jung, 2011), in weakly ionized plasma (Pandey *et al*., 2012), in relativistic hot plasma (Shaisultanov *et al.*, 2012) and in laboratory plasma (John & Sexena, 1975). During the last decades, the study of electron-positron-ion (e-p-i) plasma has a great deal of attraction studied (Popel *et al*., 1995; Salahuddin *et al.*, 2002; Roy *et al.*, 2012). The magneto hydrodynamic oscillations in astrophysics plasma with relativistic positrons and electrons were studied by (Maroof *et al.*, 2015). They revealed that the dispersive features of magneto hydrodynamic oscillations have been profoundly altered by electrons and positrons relativistic degeneracy effects. The growth rate of electron-positron-ion in two-stream instability was studied by (Saleem & Khan, 2005). Their study revealed that the growth rate depends on the ratio of constituent particles. In most of the astrophysical plasma-like pulsars, early universe, and Active Galactic Nuclei (AGN), it is assumed that it may be composed of electrons, positrons, and ions (Saleem & Khan, 2005). Helandar and Ward (Helandar & Ward, 2003) showed that the production of positron on laboratory level in devices like tokamaks is due to airstrip electrons collision with thermal electrons or ions. Based on the above argument and applications of electron-positron-ion plasma to laboratory and astrophysical environments, it looks very important to study the e-p-i instabilities in plasma and for the exact solution of the soliton structure studied in (Seyma *et al*., 2017). In recent years, the quantum hydrodynamic models become popular as a simplified but not simplistic approach for quantum plasmas. In particular, the nonlinear aspects of quantum plasmas are much more accessible using a fluid description, in comparison with kinetic theory. The full three-dimensional quantum hydrodynamic (QHD) model is derived for the first time by a moment expansion of the Wigner Boltzmann equation. The QHD conservation laws have the same form as the classical hydrodynamic equations, but the energy density and stress tensor have additional quantum terms. These quantum terms allow particles to tunnel through potential barriers and to build up in potential wells. Hydrodynamic models were developed several times in condensed matter physics, particularly for applications to semi-conductors (Bloch equations), to a lesser extent,

metal clusters, where they are frequently referred to as time-dependent Thomas-Fermi models. However, most hydrodynamic models used in the past do not contain quantum effects, apart from the Fermi-Dirac statistics. Further, the results of the hydrodynamic simulations were generally validated for the electric-dipole response and frequency spectrum, whereas higher order quantities such as the thermal and potential energies were not properly assessed. Recent numerical simulations and experiments have highlighted several interesting effects precisely involving these quantities when thin metal films are irradiated with femtosecond laser pulses most notably, ultrafast heating and ballistic oscillations of the electron gas (Hervieux & Manfredi, 2008). The primary application of various quantum hydrodynamic (QHD) equations to date has been in analyzing the flow of electrons in quantum semiconductor devices. The QHD equations, however, are quite general and may find applications in other areas of physics, e.g., fluid models of the nucleus, superconductivity, and superfluidity.

Understanding the collective dynamics of a quantum electron gas is of great importance for a large variety of physical systems, including metallic nanostructures, thin metal films, semiconductor quantum wells, and quantum dots. In particular, recent experimental progress in femtosecond pump-probe spectroscopy allowed the investigation of the electron dynamics on an ultrafast time scale, where collective effects play a crucial role (Hervieux & Manfredi, 2008). The complicated behavior of the QHD equations is not surprising, given the complexity of the underlying many-particle quantum system. On the other hand, this means that when applying QHD models to real quantum plasmas, careful applicability tests and comparisons to more accurate approaches, such as quantum kinetic theory (QKT), DFT, or quantum Monte Carlo (QMC), are indispensable. However, many papers that applied QHD models to quantum plasmas neither include a careful validity analysis nor comparisons to experiments or more accurate theories. So it does not come as a surprise that numerous predictions have been made that are either highly speculative or even in conflict with results that are well established in other fields. For this reason, these results have not been picked up by researchers outside the QHD-quantum plasma community except for occasional critical comments, Attractive forces between ions in quantum plasmas: Failure of linearized quantum hydrodynamics, For example, (Vranjes *et al*., 2012) concluded (we quote from the abstract of “The quantum plasma theory has flourished in recent years without much regard to the physical validity of the formulation or its connection to any real physical system. It is argued here that there is a very limited physical ground for the application of such a theory.

A prominent example of untested claims was the prediction of novel attractive forces between protons in equilibrium quantum plasma by Shukla and Eliasson (known as the SE potential) (Shukla & Eliasson, 2012). These predictions were proven wrong by ab initio density functional theory simulations, where also the limitations of linearized QHD were pointed out, The failure of the SE potential is also confirmed by quantum kinetic theory (Bonitz *et al*., 2019). A second prominent example of unjustified claims was the prediction of unphysical high spin polarization in quantum plasmas, the notion of spinning quantum plasmas, and the invention of "spin lasers".

In this work, we present the analysis of low frequency linear and nonlinear collisional quantum Buneman instability in electron-positron-ion plasmas. Our approach is based on the quantum hydrodynamic plasmas model to study the quantum Buneman instability in electron-positron-ion plasma which is very useful for the nonlinear problems in Quantum Coulomb systems (Haas, 2011). In our work, linear and non-linear low-frequency collisional quantum Buneman instability in electron-positron-ion plasmas are investigated, extending the Haas model (Haas & Bret, 2012) of low-frequency quantum plasma in a one-dimensional collisional system. Our main focus is on Buneman instability by including the positron effect. We shall present different possible plasma configurations based on the relative velocity of streaming particles. We organized this work in the following way. In Section 2, the basic model equations of the plasma dynamic are used for the three species cold QHD model by extending the two species cold QHD Haas model (Haas & Bret, 2012). Section 3, presents the numerical results and discussion which shows the importance of the present study, its applicability both in astrophysics and laboratory plasmas. In the same section for illustration, we present some parametric analysis. Section 4, is devoted to the summary of this work.

1. Basic Model Equations

We assumed the propagation of electrostatic waves in non-magnetized, low frequency collisional three species (electron-positron-ion) plasma. We consider a three species cold quantum hydrodynamic model by extending the two species cold quantum hydrodynamic model of Haas (Haas & Bret, 2012), taking into account the effect of positron on low-frequency quantum Buneman instability. The effect of collision and Bohm potential (quantum) terms along with the positron effect were included in the one-dimensional hydrodynamic model using simple relaxation terms.

In the fluid description, the dynamics of these particles are expressed by the following model equations.

$$\frac{\partial n_i}{\partial t} + \frac{\partial (n_i v_i)}{\partial x} = 0 \tag{1}$$

$$\frac{\partial n_e}{\partial t} + \frac{\partial (n_e v_e)}{\partial x} = 0 \tag{2}$$

$$\frac{\partial n_p}{\partial t} + \frac{\partial (n_p v_p)}{\partial x} = 0 \tag{3}$$

$$\frac{\partial v_i}{\partial t} + v_i \frac{\partial v_i}{\partial x} = \frac{qE}{m_i} - \nu_{i1} v_i \tag{4}$$

$$\frac{\partial v_e}{\partial t} + v_e \frac{\partial v_e}{\partial x} = -\frac{qE}{m_e} - v_e \nu_e + \frac{\hbar^2}{2m_e^2} \frac{\nabla_x}{2} \left(\frac{\nabla_x^2 \mathrm{n}_e}{\mathrm{n}_{e0}} \right) \quad (5)$$

$$\frac{\partial v_p}{\partial t} + v_p \frac{\partial v_p}{\partial x} = \frac{qE}{m_p} - v_p \nu_p + \frac{\hbar^2}{2m_p^2} \frac{\nabla_x}{2} \left(\frac{\nabla_x^2 \mathrm{n}_p}{\mathrm{n}_{p0}} \right) \quad (6)$$

The Poisson equation is given as,

$$\frac{\partial E}{\partial x} = \frac{q}{\epsilon_0} (n_i + n_p - n_e) \quad (7)$$

Due to the larger mass of ions ($m_e = m_i << 1$), the quantum term is not included in the ion momentum equation. In the above expressions, n is the number density, v is the fluid velocity, E is the electrostatic field, I is the mass of an electron, m_p is the mass of the positron, m_i is the ion mass, q is the charge on positron, ν_i is the collision frequencies, $\hbar = \frac{h}{2\pi}$ where his Planks constant and ϵ_0 is the permittivity of free space (vacuum).

To get the linearized dispersion relation based on our model equation we consider first order perturbation such that $n_i = n_{i0} + n_{i1}, n_e = n_{e0} + n_{e1}, n_p = n_{p0} + n_{p1}, v_i = v_{i0} + v_{i1}, v_e = v_{e0} + v_{e1}, \; v_p = v_{p0} + v_{p1}, and \; E = E_0 + E_1,$ where the subscripts 0 and 1 represent background and perturbed quantities respectively. Background electric field (external DC) and ion background velocity v_{i0} are taken to be zero at equilibrium. In small amplitude limits by supposing the perturbations $\sim \exp(\iota|k_x - \omega t|)$ with the wave frequency ω wavenumber k, linearizing the model equations around the homogenous equilibrium requires the charge neutrality condition which is $n_{i0} + n_{p0} = n_{e0} = n_0$, we can write,

$$n_{i1} = \frac{ik}{mi} \frac{qE_1}{\omega(\omega + i\nu_i)} n_{i1} \quad (8)$$

$$n_{e1} = -\frac{ik}{me} \left(\frac{n_0 q E_1}{(\omega - k v_{e0})(\omega - k v_{e0} + i\nu_e) - \frac{\hbar^2 k^2}{4m_e^2}} \right) \quad (9)$$

$$n_{p1} = \frac{ik}{mp} \left(\frac{n_{p0} q E_1}{(\omega - k v_{p0})(\omega - k v_{p0} + i\nu_p) - \frac{\hbar^2 k^2}{4m_p^2}} \right) \quad (10)$$

Using equations (8-10) in the Poisson equation (7), after simplification, we obtain the following dispersion relation,

$$1 - \frac{\omega_{pi}^2}{\omega(\omega + i\nu_i)} -$$

$$\omega_{pe}^2 \left(\frac{\delta_n}{(\omega - k v_{p0})(\omega - k v_{p0} + i\nu_p) - \frac{\hbar^2 k^2}{4m_p^2}} + \frac{1}{(\omega - k v_{e0})(\omega - k v_{e0} + i\nu_e) - \frac{\hbar^2 k^2}{4m_e^2}} \right) = 0 \quad (11)$$

Where $\delta_n = \frac{n_p}{n_0}$ is the ratio of positron to electron number density at equilibrium. $\omega_{pe}^2 = \frac{n_0 q^2}{\epsilon_0 m_e}$ is the electron plasma frequency and the ion plasma frequency $\omega_{pi}^2 = \frac{n_{i0} q^2}{\epsilon_0 m_i}$.
Using the conditions of low frequency $\omega \ll v_i \ll kv_{i0}\ and\ v_{e0} \ll kv_{e0}\ and\ v_{p0} \ll kv_{p0}$ the above equation reduces to

$$\omega = i\frac{\omega_{pi}^2}{\nu_i}\begin{pmatrix} \frac{k^2(v_{p0}^2-\frac{\hbar^2k^2}{4m^2})(v_{e0}^2-\frac{\hbar^2k^2}{4m^2})}{\omega_{pe}^2(\delta_n\left((v_{e0}^2-\frac{\hbar^2k^2}{4m^2}\right)+\left(v_{p0}^2-\frac{\hbar^2k^2}{4m^2}\right)} \\ -k^2(v_{p0}^2-\frac{\hbar^2k^2}{4m^2})(v_{e0}^2-\frac{\hbar^2k^2}{4m^2}) \end{pmatrix} \quad (12)$$

If one ignores the positron effect it gets the shape given in (Haas & Bret, 2012),

$$\omega = i\frac{\omega_{pi}^2}{\nu_i}\left(\frac{k^2(v_{e0}^2-\frac{\hbar^2k^2}{4m^2})}{\omega_{pe}^2-k^2v_{e0}^2-\frac{\hbar^2k^{42}}{4m^2})}\right) \quad (13)$$

Equation (13) gives us the same result for electron ion plasmas in (Haas & Bret, 2012).
In order to find out the growth rate we consider the following normalized parameters

$t \rightarrow \frac{\omega_{pi}^2}{\nu_i}t,\ x \rightarrow \frac{\omega_{pe}^2}{v_0}x, v_p \rightarrow \frac{v_p}{v_0}, v_i \rightarrow \frac{\nu_i m_i v_i}{m\omega_{pe}v_0}, n_i = n_0\ n_i\ , n_e = n_0\ n_e\ ,$

$n_p = n_0\ n_p\ , and\ E = \frac{eE}{m\omega_{pe}v_0}$. Using the above transformations in the basic model equations. (1-7), we get the following normalized set of equations as

$$\frac{\omega_{pi}^2}{\omega_{pe}^2}\frac{\partial n_i}{\partial t} + \frac{\partial(n_i v_i)}{\partial x} = 0 \quad (14)$$

$$\frac{\omega_{pi}^2}{\nu_i\omega_{pe}^2}\frac{\partial n_e}{\partial t} + \frac{\partial(n_e v_e)}{\partial x} = 0 \quad (15)$$

$$\frac{\omega_{pi}^2}{\nu_i\omega_{pe}^2}\frac{\partial n_p}{\partial t} + \frac{\partial(n_p v_p)}{\partial x} = 0 \quad (16)$$

Using the values of $\omega_{pe}^2\ and\ \omega_{pi}^2$ in the equation (14), we have

$$\alpha_n\frac{\partial n_i}{\partial t} + \frac{\partial(n_i v_i)}{\partial x} = 0 \quad (17)$$

Where $\alpha_n = \frac{n_{i0}}{n_{e0}}$is the ratio of background ion to electron number density. Similarly, the momentum equations for ions, electrons and positrons can be written as under

$$\frac{\omega_{pi}^2}{v_i^2}\frac{\partial v_i}{\partial t} + v_i\frac{\partial v_i}{\partial x} = E - v_i \tag{18}$$

$$\frac{\omega_{pi}^2}{v_i\omega_{pe}}\left(\frac{\partial v_e}{\partial t} + v_e\frac{\partial v_e}{\partial x}\right) =$$

$$-E - \frac{v_e}{\omega_{pe}}v_e \; + \frac{H^2}{2}\,\frac{\nabla_x}{2}\left(\frac{\nabla_x^2 \mathrm{n}_e}{\mathrm{n}_{e0}}\right) \tag{19}$$

$$\frac{\omega_{pi}^2}{v_i\omega_{pe}}\left(\frac{\partial v_p}{\partial t} + v_p\frac{\partial v_p}{\partial x}\right) =$$

$$E - \frac{v_p}{\omega_{pe}}v_p + \frac{H^2}{2}\,\frac{\nabla_x}{2}\left(\frac{\nabla_x^2 \mathrm{n}_p}{\mathrm{n}_{p0}}\right) \tag{20}$$

And the Poisson equation in normalized form as

$$\frac{\partial E}{\partial x} = \frac{q}{\epsilon_0}(\, n_i + \, n_p - n_e \,) \tag{21}$$

Where H= $\frac{\hbar^2\omega_{pe}}{m\mathrm{v}_0^2}$ is the dimensionless parameter that measure the weight of Bohm potential. Provided the limiting conditions that $v_i \gg \omega_{pi}$ and $\omega_{pe} \gg v_e$, the normalized model equations can be written as

$$n_{e0}\frac{\partial v_{e1}}{\partial t} + v_{e0}\frac{\partial n_{e1}}{\partial x} = 0 \tag{22}$$

$$n_{p0}\frac{\partial v_{p1}}{\partial t} + v_{p0}\frac{\partial n_{p1}}{\partial x} = 0 \tag{23}$$

$$\alpha_n\frac{\partial n_{i1}}{\partial t} + n_{i0}\frac{\partial v_{i1}}{\partial x} = 0 \tag{24}$$

$$v_i = E_1 \tag{25}$$

$$\frac{\partial v_{e1}}{\partial x} = -E \; + \frac{H^2}{2}\,\frac{\nabla_x}{2}\left(\frac{\nabla_x^2 \mathrm{n}_{e1}}{\mathrm{n}_{e0}}\right) \tag{26}$$

$$v_{p0}\frac{\partial v_{p1}}{\partial x} = E \; + \frac{H^2}{2}\,\frac{\nabla_x}{2}\left(\frac{\nabla_x^2 \mathrm{n}_{p1}}{\mathrm{n}_{p0}}\right) \tag{27}$$

$$\frac{\partial E}{\partial x} = \; n_i + \; n_p - n_e \tag{28}$$

After linearizing the above equations.
(22-28) and some standard manipulation leads to

$$n_{i1} = \frac{kE_1}{\omega} n_{i0} \tag{29}$$

$$n_{e1} = -i \frac{n_{e0} E_1}{k\left(v_{e0}^2 - \frac{H^2k^2}{4}\right)} \tag{30}$$

$$n_{p1} = i \frac{n_{p0} E_1}{k\left(v_{p0}^2 - \frac{H^2k^2}{4}\right)} \ , \tag{31}$$

Using equations. (29-31) in equation (28) leads to the following dispersion relation

$$\omega = i \left(\frac{n_0 k^2 (v_{p0}^2 - \frac{H^2k^2}{4})(v_{e0}^2 - \frac{H^2k^2}{4})}{n_{p0}((v_{e0}^2 - \frac{H^2k^2}{4}) - n_{e0}(v_{p0}^2 - \frac{H^2k^2}{4})} \right) \tag{32}$$
$$-k^2 (v_{p0}^2 - \frac{H^2k^2}{4})(v_{e0}^2 - \frac{H^2k^2}{4}))$$

Using $\omega = \omega_R + i\gamma$ and the background neutrality condition, we have the relation for growth rate

$$\gamma = \frac{k^2 (v_{p0}^2 - \frac{H^2k^2}{4})(v_{e0}^2 - \frac{H^2k^2}{4})}{n_{p0}(v_{e0}^2 - \frac{H^2k^2}{4}) - (v_{p0}^2 - \frac{H^2k^2}{4})} \tag{33}$$
$$-k^2 (v_{p0}^2 - \frac{H^2k^2}{4})(v_{e0}^2 - \frac{H^2k^2}{4})$$

2. Numerical results and discussion

For numerical results and discussion, we study the quantum effect of the parameter H on growth rate γ for two possible electron-positron-ion plasma configurations. For these configurations, different types of cases like classical, semi-classical, and pure quantum cases are numerically solved and plotted. These types of configurations are based on the constituent particles relative velocities. Such configurations may exist in pulsars, AGN, and experimental plasma. Equation (33) is general dispersion relation, which can be extended to other possible configurations.

3.1 Configuration 1:

In this configuration electrons-positrons fluid moves with constant velocity v_0 relative to ions. Putting $v_{p0} = v_{e0} = v_0 = 1$ as we normalized the electrons and positrons fluids velocity with respect tov_0, then equation. (33) gives w.r.t v_0

$$\gamma = \frac{k^2 (1 - \frac{H^2k^2}{4})}{n_{p0} - 1 - k^2 (1 - \frac{H^2k^2}{4})} \tag{34}$$

The quantum effect of the parameter H on growth rate with different positron concentrations is plotted. Normalized variables to study the different cases like classical, semi-classical, and pure quantum cases. In Figure 1. We showed the effect of positron number density on the growth rate. In classical case (H = 0), we have

$\gamma = \frac{k^2}{1+n_{p0}-k^2}$. The denominator in the quadratic equation where the positive value of k is 1 < k < 1.6 and linear instability were found in this region. The vertical asymptotes vary with positron concentration and point explosive instability, at k =1 for low positron concentration (0.1) and at k = 1.5 for high positron concentration. In all figures the red dashed line shows n_p = 0.1, the blue dotted line shows n_p = 0.5 and the green line shows n_p = 0.9.

In semi-classical case (0 < k < 1) the growth rate from equation. (34) has two asymptotes at $k_{A, B}$. The behavior of growth rate as a function of wavenumber k is shown in Figure 2. In special case H = 1 the mid stable part disappears although instability exists in 0 < k < 1.6 region. The maximum growth rate shrinks to zero for higher positron concentrations. This behavior is shown in Figure 3 which shows stabilizing nature of positron at the quantum level. In pure quantum case H > 1 the maximum growth rate shrink to zero for any positron concentration. This shows the stabilizing nature of quantum effects. This behavior is shown in Figure 4.

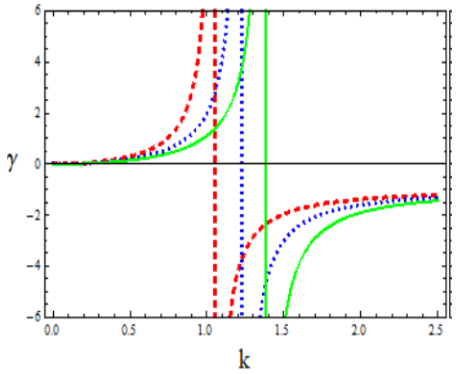

Fig. 1. The growth rate γ in equation (34) in terms of wave number (k), in classical. Limit (H = 0). In-stability is found at 0 < k < 1 for lower positron concentration and at 0 < k < 1.6 for higher positron concentration. The red dashed line shows n_p= 0.1, the blue dotted line shows n_p= 0.5 and the green line shows n_p= 0.9.

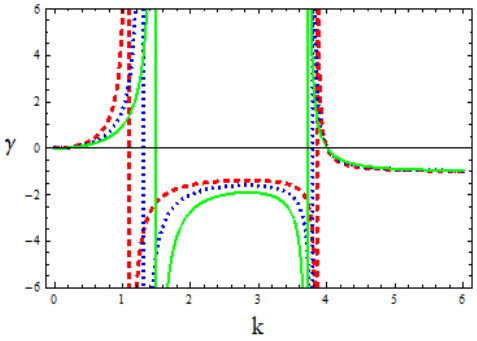

Fig. 2. The growth rate γ in equation (34) in terms of wave number (k), in semi classical. Limit (0 < H <1). Instability is found at 0 < k < kA for lower positron concentration and at kB < k < kC.The red dashed line shows n_p= 0.1, the blue dotted line shows n_p= 0.5 and the green line shows n_p= 0.9.

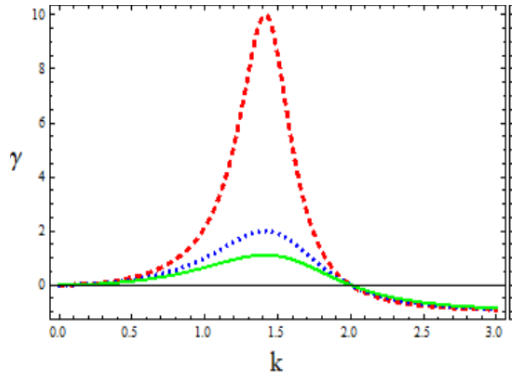

Fig. 3. The growth rate γ in equation (34) in terms of wave number (k), in quantum. Limit (H = 1). Instability is found at 0 < k < 2. The red dashed line shows n_p = 0.1, the blue dotted line shows n_p = 0.5and the green line shows n_p = 0.9.

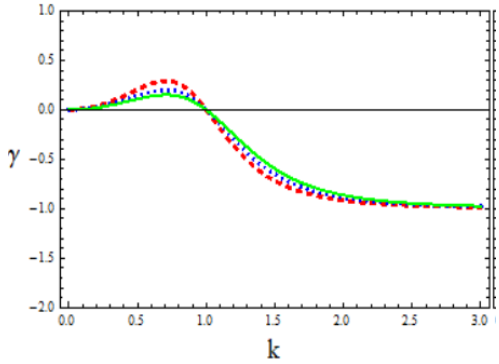

Fig. 4. The growth rate γ in equation (34) in terms of wavenumber (k), in pure quantum Limit (H =2). Instability is found at 0 < k < 1.6. The red dashed line shows n_p = 0.1, the blue dotted line shows n_p = 0.5 and the green line shows n_p = 0.9.

3.2. Configuration 2:

In this configuration positrons fluid moves with constant velocity v_0 relative to electrons-ions fluid. Putting v_{e0} =0 and $v_{p0} = v_0$ =1 as we normalized the electrons and positrons fluids velocity with respect to v_0

$$\gamma = \frac{k^2\left(v_{p0}^2-\frac{H^2k^2}{4}\right)\left(-\frac{H^2k^2}{4}\right)}{n_{p0}\left(-\frac{H^2k^2}{4}\right)-\left(v_{p0}^2-\frac{H^2k^2}{4}\right)-k^2\left(v_{p0}^2-\frac{H^2k^2}{4}\right)\left(-\frac{H^2k^2}{4}\right)} \tag{35}$$

The effect of quantum parameter H on growth rate with different positron concentrations was shown. Different cases like classical, semi-classical, and pure quantum cases are discussed. In the Classical case H = 0, putting this one can get $\gamma = 0$. In semi-classical cases, the asymptotes point to explosive instability at k = 4. The maximum growth rate shifted toward a higher value of k. The behavior of growth rate γ as a function of wavenumber k is shown in Figure 5. In spatial case H = 1 the maximum growth rate shifted towards the lower value of k. Instability was found

at $0 < k < 2$. This behavior is shown in Figure 6. In the pure quantum region ($H = 2$) the growth rate again shifted towards a lower value of k. Instability is found at $0 < k < 1$. This behavior is shown in Figure 7.

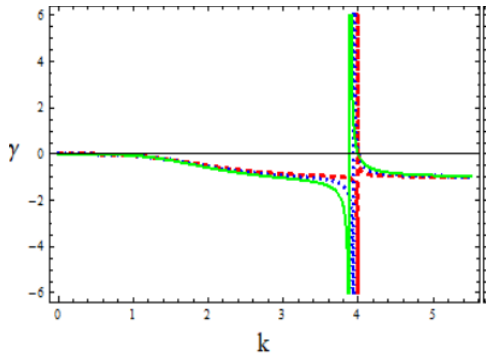

Fig. 5. The growth rate γ in equation (35) in terms of wave number (k), in pure quantum. Limit ($H = 0.5$). Instability is found at $0 < k < 4$: The red dashed line shows $n_p = 0.1$, the blue dotted line shows $n_p = 0.5$ and the green line shows $n_p = 0.9$.

Fig. 6. The growth rate γ in equation (35) in terms of wave number (k), in special. Limit ($H = 1$). Instability is found at $0 < k < 2$: The red dashed line shows $n_p = 0.1$, the blue dotted line shows $n_p = 0.5$ and the green line shows $n_p = 0.9$.

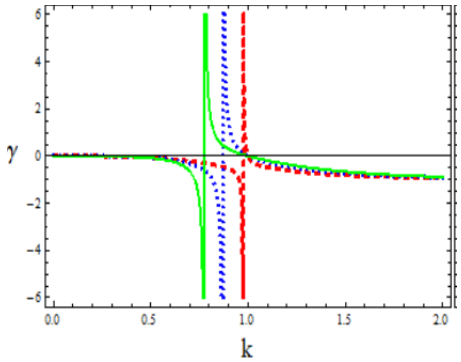

Fig. 7. The growth rate γ in equation (35) in terms of wavenumber (k), in strong quantum. Limit ($H = 2$). Instability is found at $0 < k < 1$: The red dashed line shows $n_p = 0.1$, the blue dotted line shows $n_p = 0.5$ and the green line shows $n_p = 0.9$.

3. Summary

The non-linear growth of low-frequency collisional quantum Buneman instability in e-p-i plasma was studied both numerically and parametrically, through one dimensional model for two possible streaming configurations. It is found that when electrons-positrons fluid moves with constant velocity relative to ions fluid, at classical and semi-classical limits (H = 0 and H = 0.5) respectively, the positron concentration enhances the unstable region but at quantum limits, the increasing positron concentration shrinks the maximum growth rate and unstable region to zero. For such type of a configuration in which electron-ion plasma is at rest relative to positrons fluid, it is found that positrons fluid causes an increase in the unstable region in classical limits however this region was found to reduce for purely quantum plasma.

4. Financial and Ethical disclosures

This study is not funded by any source, or any company and it is carried by the authors themselves. Since none of the authors has received any honorarium from any company, therefore the authors have no conflict of interest.

References

Bandara, R. & Khachan, J. (2013). Spherical ion oscillations in a positive polarity gridded inertial-electrostatic confinement device, Physics of Plasmas (1994- present), 20: 072705.

Bonitz, M., Moldabekov, Zh. A. & Ramazanov, T. S. (2019). Quantum hydrodynamics for plasmas—Quo vadis, Physics of Plasmas 26: 090601.

Buneman, O. (1958). Instability, Turbulence, and Conductivity in Current-Carrying Plasma, Physical Review, 1: 119.

Buneman, O. (1959). Dissipation of current in ionized Media, Physical Review, 115(**3**): 503.

Dolgov, S. V., Smirnov, A. P. & Tyrtyshnikov, E. E. (2014). Low-rank approximation in the numerical modeling of the Farley-Buneman instability in ionospheric plasma, Journal of Computational Physics, 263: 268-282.

Haas, F. (2011). Quantum Plasmas, a Hydrodynamic Approach (Springer New York), 65: 1-220.

Haas, F. & Bret, A. (2012). Nonlinear low-frequency collisional quantum Buneman instability, EPL (EuroPhysics Letter), 97(**2**): 26001.

Haas, F., Eliasson, B. & Shukla, P. K. (2012). Negative energy waves and quantum relativistic Buneman instabilities, Physical Review E, 86(**3**): 036406.

Helandar, P. & Ward, D. J. (2003). Positron creation and annihilation in tokamak plasmas with runaway electrons, Physical Review Letters, 90(**13**): 135004.

Hervieux, P. A. & Manfredi, G. (2008). Quantum hydrodynamic model for the nonlinear electron dynamics in thin metal films, Physical Review B 78: 155412.

Hong, W. P. & Jung, Y. D. (2015). Influence of the oscillatory quantum screening on the occurrence scattering time in electron-ion quantum plasmas, Physics of Plasmas 19: 024506.

Inhester, B., Das, AC. & Fejer, J. A. (1981). Generation of small-scale field-aligned irregularities in ionospheric heating experiments, Journal of Geophysical Research Space Physics, 86 (**A11**): 9101-9106.

John, P. I. & Saxena, Y. C. (1975). Observation of the Farley-Buneman Instability in laboratory plasma, Geophysical Research Letters, 2(**6**): 251-254.

Jun, Gou. & Bin, Yu. (2012). Competition between Buneman and Langmuir Instabilities, Chinese Physics Letters, 29(3): 035203.

Ki, D., H. & Jung, Y. D. (2011). Nonthermal effects on the Buneman instability in Lorentzian dusty plasmas Physics of Plasmas, 18(**1**): 014506.

Madsen, C. A., Dimant, Y. A. Oppenheim, M. M. & Fontenla, J. M. (2012). Quantum quench dynamics in cold atom systems, in APS Meeting Abstract, and volume 57(**1**): page 8043P.

Madsen, C. A., Dimant, Y. S., Oppenheim, M. M. & Fontenla, J. M. (2014). The multispecies Farley-Buneman instability in the solar chromosphere, The Astrophysical Journal, 783(**2**): 128.

Maroof, R., Ali, S., Mushtaq, A. & Qamar, A. (2015). Magnetohydrodynamic waves with relativistic electrons and positrons in degenerate spin-1/2 astrophysical plasmas, Physics of. Plasmas (1994- Present), 22(**11**): 112102.

Niknam, AR., Komaiz, D. & Hashemzadeh, M. (2011). Self-focusing and defocusing of Gaussian laser beams in collisional inhomogeneous plasmas with linear density and temperature ramps, Physics of Plasmas (1994-present), 18(**2**): 022301.

Pandey, B. P. & Vladimirov, S. V. (2012). Farely- Buneman instability in weakly ionized Medium, In Plasma Science (ICOPS) Abstracts IEEE International Conference, pages 2P- 32, IEEE.

Pandey, S. & Bhattacharjee, S. (2014). Observation of ion heating during stimulated Buneman instability in a temporally growing plasma, EPL (Euro Physics Letter), 108(**1**): 15001.

Popel, S. I., Vlandimirow, S. V. & Shukla, P. K. (1995). Ion-acoustic solitons in electron–positron–ion plasmas, Physics of Plasmas, (1994-present) 2(**3**): 716-719.

Roy, N., Tasnim, S. & Mamun, A. A. (2012). Solitary waves and double layers in an ultra-relativistic degenerate dusty electron-positron-ion plasma, Physics of Plasmas (1994-present), 19(**3**): 033705.

Salahuddin, M., Saleem, H. & Saddiq, M. (2002). Ion-acoustic envelope solitons in electron-positron-ion plasmas, Physical Review E, 66(**3**): 036407.

Saleem, H. & Khan, R. (2005). Two-Stream Instabilities in Electron–Positron–Ion Plasmas, Physica. Scripta, 71(**3**): 314.

Seyma, T. D. & Hasan Bulut (2017). New exact solutions for generalized Gardner equation, Kuwait Journal of Science, Vol 44(**1**).

Shaisultanov, R., Lyubarsky, Y. & Eichler, D. (2012). Streaming instability in reletivistically hot plasma, The Astrophysical Journal, 744(**2**): 182.

Shokri, B. & Niknam, AR. (2005). Nonlinear dynamic of low-frequency Buneman instability of a current-driven plasma, Physics of Plasmas (1994-present), 12(**6**): 062110.

Shukla, P. K. & Eliasson B. (2012). Novel Attractive Force between Ions in Quantum Plasmas, Physics Review Letters. 108:165007.

Vranjis, J., Pandey, B. P. & Poedts, S. (2012). On quantum plasma: A plea for a common sense, EPL (EuroPhysics Letter) 99 (**2**): 25001.

Submitted: 18/12/2020
Revised: 07/12/2020
Accepted: 08/12/2020
DOI: 10.48129/kjs.v49i1.10547